Post-print of: Mroziński A., Molin S., Karczewski J., Kamecki B., Jasiński P.: The Influence of Iron Doping on Performance of SrTi1-XFexO3-δ Perovskite Oxygen Electrode for SOFC. ECS Transactions. Vol. 91, iss. 1 (2019), pp. 1299-1307. DOI: 10.1149/09101.1299ecst

# The influence of Iron Doping on Performance of $SrTi_{1-x}Fe_xO_{3-\delta}$ Perovskite Oxygen Electrode for SOFC

A. Mroziński[a], S. Molin[a], J. Karczewski[b], B. Kamecki[b], and P. Jasiński[a]

[a] Laboratory of Functional Materials, Faculty of Electronics, Telecommunications and Informatics, Gdańsk University of Technology, Gdańsk 80-233, Poland
[b] Department of Solid State Physics, Faculty of Applied Physics and Mathematics, Gdańsk University of Technology, Gdańsk 80-233, Poland

Solid Oxide Fuel Cells (SOFC) are based on electrolytes and mixed ionic and electronic conductivity (MIEC) materials. The need to reduce costs causes an increase in interest of new compounds suitable for operating temperatures between 600 °C and 800 °C. The $SrTi_{1-x}Fe_xO_3$ (STF) perovskite material is a perspective material that could be used for the oxygen electrodes. In this work STF materials with different content of iron (x = 0.35, 0.5 and 0.7) have been evaluated. The paper presents synthesis, sintering properties, paste and layer preparation with preliminary electrical measurements. The results show that the electrical conductivity increases with the addition of iron, whereas the activation energy decreases. Based on these results, the applicability of STF as a potential oxygen electrode was discussed.

## Introduction

Presently the materials with mixed ionic and electronic conductivity (MIEC) are widely used in different electrochemical systems for energy conversion, e.g. Solid Oxide Fuel Cells (SOFC). Typical operating temperature of the efficient SOFC is above 800 °C and it is caused by the sluggish oxygen reaction rate (ORR) of the cathode material (1). Therefore, high performance new materials for the oxygen electrodes operating at the temperatures range between 600 °C and 800 °C are sought. Most of the investigated MIEC cathodes belongs to the perovskites group including a perspective $SrTi_{1-x}Fe_xO_{3-\delta}$ (STF) (2). Pure undoped $SrTiO_3$ (STO) is a model MIEC material (3) with a low electronic and high oxygen ionic conductivity (4). The defect chemistry of the STO oxide shows that by an iron doping it is possible to increase the electronic conductivity at a cost of ionic conductivity, without changing an oxygen surface exchange mechanism (5,6). Unfortunately pure $SrFeO_3$ (SFO) is not compatible material for SOFC, because of phase transition at about 830 °C. Therefore STF compounds with different amount of iron dopant are gaining more and more interest for evaluation as material for SOFC (7).

One of a common and cheap techniques to synthesize STF frequently utilized in literature is a solid state reaction (SSR) method. The prepared powder can be used in different ways e.g. as an electrode, oxygen sensor or oxygen membrane (8,9). Another possibility to fabricate STF electrode is Pulsed Laser Deposition (PLD). For PLD technique there is needed for a laser beam and pre synthesized target of a metals oxides. By using pulsed laser, metals/metal oxides from target are deposited onto substrates (10,11). Alternative method for PLD are spin-coating or spray pyrolysis. For these

methods nitrates solutions of metals are used as a precursors. From nitrates a STF powder can be prepared as well (12–14). Comparing all this techniques, the traditional SSR method is the easiest and the cheapest one with high repeatability.

This work focuses on the STF compounds with different content of iron dopant (x = 0.35; 0.5; 0.7) made by SSR method. In this study material characterization of the prepared STF and preliminary results of DC electrical conductivity of a dense STF materials and porous STF layers deposited by screen printing method onto $Al_2O_3$ substrates are shown.

## Experimental

### Samples fabrication

In this study, the STF material with three different levels of iron (x = 0.35; 0.5 and 0.7) were prepared. The compounds were fabricated by conventional high temperature SSR method. The analytical reagents used for the reaction were strontium carbonate ($SrCO_3$), titanium dioxide ($TiO_2$) and iron (III) oxide ($Fe_2O_3$). The first two were purchased from the EuroChem (PL) and third from the Chempur (PL). Syntheses of the STF materials were described in more details in our previous work (2). The obtained $SrTi_{0.65}Fe_{0.35}O_{3-\delta}$ (STF35), $SrTi_{0.5}Fe_{0.5}O_{3-\delta}$ (STF50) and $SrTi_{0.3}Fe_{0.7}O_{3-\delta}$ (STF70) materials, after re-grounding in a mortar were ball milled (Fritsch Pulverisette 7) in ethanol (99.9% purity) with rotational speed of 600 rpm for 15 h using the 5 mm YSZ balls.

The DC electrical conductivity measurements were made on the STF materials in two different forms: pellets and layers. The STF pellets were prepared as shown in our previous work (2). After sintering pellets had diameter of 12 mm and 94% of theoretical density, as measured by Archimedes method. Porous STF layers were fabricated on the aluminum oxide ($Al_2O_3$) substrates (Rubalit®708 S, CeramTec, DE) using the screen printing method. Before use, $Al_2O_3$ plates were washed in an acetone by an ultrasound cleaning bath. Screen printing pastes of the STF compounds for were prepared by mixing in ball mill (with 200 rpm) the STF powder and the commercial vehicle system ESL403 (Electro-Science Laboratories, USA). Mass ratio of the powder and the vehicle was 40:60. In order to prevent forming cracks of the layers during paste drying, milled STF powder were thermally processed at 600 °C (with cooling/heating rate 3° $min^{-1}$) before mixing with vehicle. After screen printing of each layer, pastes were slowly dried at 60 °C and at 130 °C. At the end samples with different number of layers (from n = 1 to n = 4) were sintered at 800 °C in air as shown in previous work (2). The achieved electrodes have diameter of 0.4 $cm^2$.

### Measurements

The X-ray diffractometry (XRD) characterization of STF powders were made at room temperature in air using Bruker D2 PHASER with XE-T detector.

Linear Thermal Expansion measurements were made in air using Netzsch DIL402. The STF compounds were heat up to 1100 °C with heating rate 5° $min^{-1}$, dwelled for 15 min and then cooled with rate of 3°C $min^{-1}$.

FEI Quanta FEG 250 Scanning Electron Microscope (SEM) were used for imaging of the STF samples. For imaging of the STF powder SEM were operated with secondary

electron (SE) detector, while for polished cross sections with backscattered electron (BSE) detector. An applied accelerating voltage was 20 kV in a high vacuum for all cases.

DC electrical conductivity measurements of the STF pellets and layers were performed as shown in previous work (2) using a Van der Pauw technique.

## Results and Discussion

Material characterization

To confirm fabrication of a perovskite cubic oxide phase of STF powders used for screen printing method, XRD analysis was made. The XRD patterns of the STF35, STF50 and STF70 powders measured at room temperature in air are shown in Fig. 1.

Identification of all diffraction peaks for STF50 and STF70 confirm that fabricated compounds has a cubic crystal structure ($Pm\bar{3}m$ ) (Inorganic Crystal Structure Database #186710) typical for strontium titanate. In case of STF35, beside cubic crystal structure peaks, there is additional one peak at 2θ = 25.6° (*). It was found, that it is related to Magnéli phase ($TiO_2$). As we reported earlier, this phase is connected with strontium nonstoichiometry (Sr/Ti < 1 in $SrTiO_3$) and does not affect the electronic conductivity of the STF compounds (2).

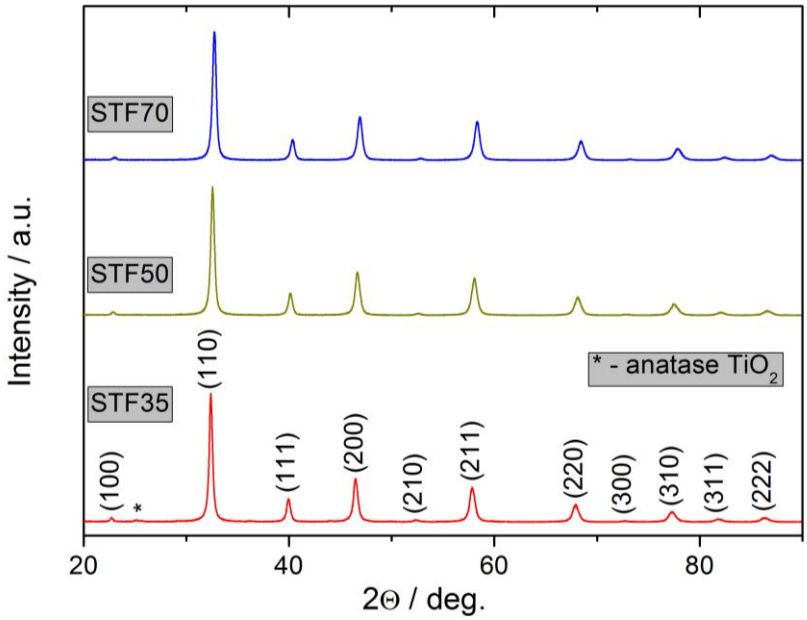


Figure 1. The XRD patterns of the fabricated STF powders for screen printing.

Dilatometry results obtained during heating up to 1100 °C (in air) of the STF powders used for screen printing are shown at Fig. 2A. The shrinkage of 0.36%, 0.38% and 0.45% of the initial length was recorded at 800 °C for STF35, STF50 and STF70, respectively. Figure 2B presents linear thermal expansion during cooling of the STF powders. The calculated thermal expansion coefficient (TEC) in the range from 1000 °C to 20 °C is 16.7 ppm $K^{-1}$, 17.9 ppm $K^{-1}$ and 23.0 ppm $K^{-1}$ for iron dopant of 0.35, 0.5 and 0.7, respectively. Based on surface morphology of sintered layers (data not shown) at different temperatures (800 °C, 900 °C and 1000 °C), it was found that rate of shrinkage

obtained at 800 °C is acceptable for preparing layers without cracks for all evaluated STF compounds, despite of so high TEC value.

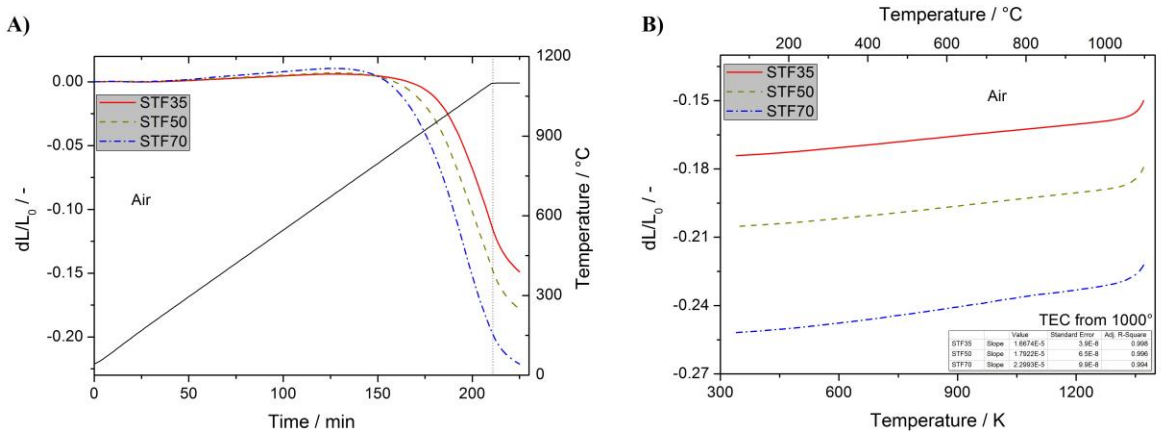


Figure 2. Temperature dependence of relative linear thermal expansion during heating (A) and cooling (B) of the fabricated STF powders.

Figure 3 shows SEM images of the STF powder used for screen printing method. It can be observed that particles of all STF powders look similar. It has been found that diameter of particles is in range from 16 nm to 140 nm. What is more, range of particle size is same as before thermal processing (data not shown), which was made to prevent cracking during drying of the STF paste.

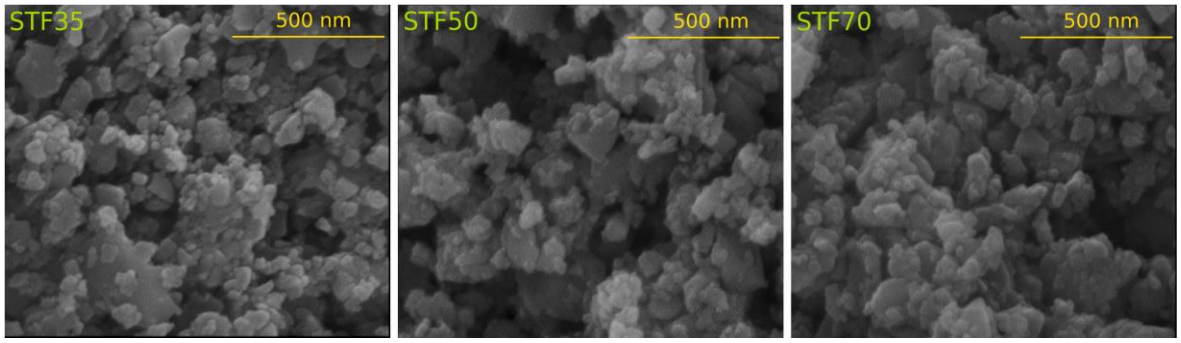


Figure 3. The SEM images of the fabricated STF powder for screen printing.

Results of DC electrical conductivity measurements of the STF dense pellets sintered at 1200 °C, are shown in Fig. 4 as a function of temperature (from 900 °C to 200 °C). The electrical conductivity investigation was conducted in synthetic air (20% $O_2$). The conductivity of the STF compounds increase with an iron dopant as expected (10). Maximum measured conductivity for STF35, STF50 and STF70 of 0.83 S $cm^{-1}$, 2.74 S $cm^{-1}$ and 19.8 S $cm^{-1}$ was obtained, respectively. With increasing of iron dopant there is observed decrease of the temperature at which maximum of conductivity appears. Namely, 850 °C, 650 ° and 600 °C was recorded for iron dopant of 0.35, 0.50 and 0.70, respectively. For the STF35 and STF50 between 900 °C and 700 °C the conductivity only slightly depend on temperature in contrast to STF70 which conductivity increase with decreasing temperature in this temperature range. The calculated activation energy at low temperatures range (400 °C ÷ 200 °C) for STF35 and STF50 are similar ($E_a$ = 33.8 kJ $mol^{-1}$ and 32.7 kJ $mol^{-1}$, respectively) but for STF70 the value is much lower ($E_a$ = 22.6 kJ $mol^{-1}$).

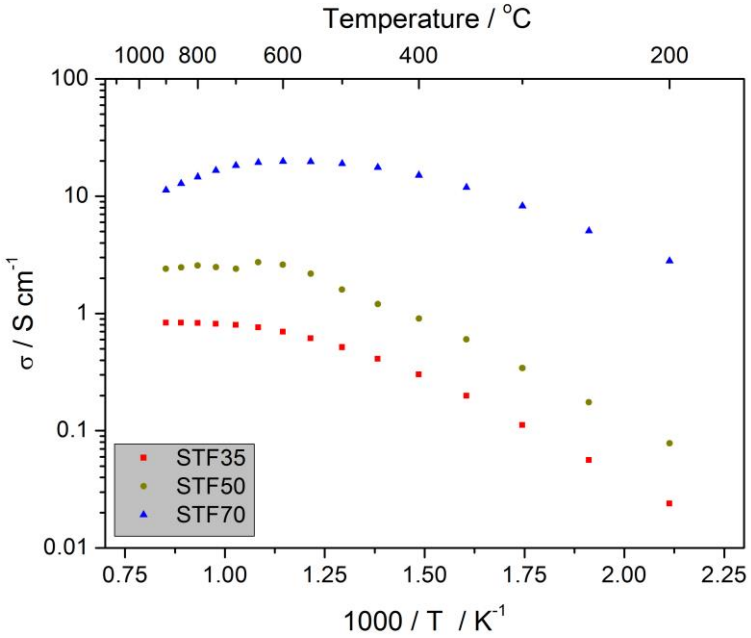


Figure 4. The DC conductivity of the dense STF pellets in function of temperature measured in 20% $O_2$.

Figure 5A presents post mortem SEM image of polished cross section of dense STF50 pellet used for DC electrical conductivity measurements. The other two STF compounds (STF35 and STF70) looked similarly (data not shown). Using the Archimedes method it was determined that this STF pellets had 94% of theoretical density. Figure 5B shows EDX spectrum of this bulk STF pellets used for conductivity measurements. EDX analysis confirmed chemical composition of investigated materials. Atomic percentage of all presented elements (Sr, Ti, Fe and O), are listed in the Table 1. All STF materials have detected deficiency of Sr atoms in the A sublattice equal 0.93.

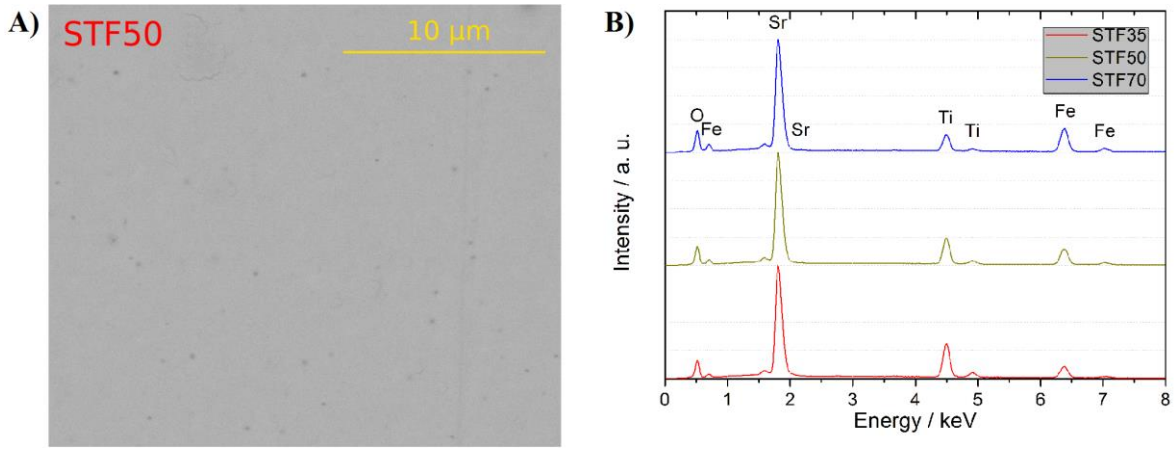


Figure 5. The SEM image of the polished cross section of the dense STF50 pellet (A) and EDX spectra of dense STF pellets used for DC conductivity measurements (B).

**TABLE I.** Chemical composition (in at.%) of dense STF pellets used for DC electrical conductivity measurements.

| | Sr | Ti | Fe | O | Sr/Ti |
|---|---|---|---|---|---|
| STF35 | 20.4 | 14.4 | 7.5 | 57.7 | 1.42 |
| STF50 | 20.9 | 11.3 | 11.1 | 56.7 | 1.85 |
| STF70 | 21.3 | 6.8 | 15.8 | 56.1 | 3.13 |

Porous layers

In order to determine influence of the STF porous electrode thickness on electrical conductivity due to chemical reaction or roughness, a DC electrical conductivity study of the electrode with different thicknesses was performed. Figure 6A shows results of DC electrical conductivity measurements of porous STF50 material in the form of layers with different thicknesses. Layers of STF50 were sintered at 800 °C that can provide little shrinkage (<1%) and at which no cracks are obtained and layers have sufficient mechanical strength. The electrical conductivity was investigated as a function of temperature (from 800 °C to 200 °C) and was conducted in synthetic air (20% $O_2$). Maximum electronic conductivity for all porous STF50 samples was recorded at 700 °C. The highest value of conductivity was obtained for porous STF50 with four layers and it is 0.11 S $cm^{-1}$. Up to 400 °C conductivity is slightly increasing with the number of layers ($\Delta\sigma \approx 0.002$ S $cm^{-1}$ $n^{-1}$). A significant change ($\Delta\sigma = 0.01$ S $cm^{-1}$) in conductivity at 700 °C is visible between samples with two and three layers. The calculated activation energy between 400 °C and 200 °C is comparable for all thicknesses and it equal $E_a = 22.3$ kJ $mol^{-1}$. At Fig. 6B is presented comparison of DC electrical conductivity of STF pellet and porous STF50 layer (n = 4). The maximum conductivity occurs almost at the same temperature (650 °C ÷ 700 °C) despite of different forms of material and temperatures of calcination. Twenty times higher conductivity for dense STF50 pellet and higher activation energy than for porous layer is probably a consequence of different calcination temperature and porosity.

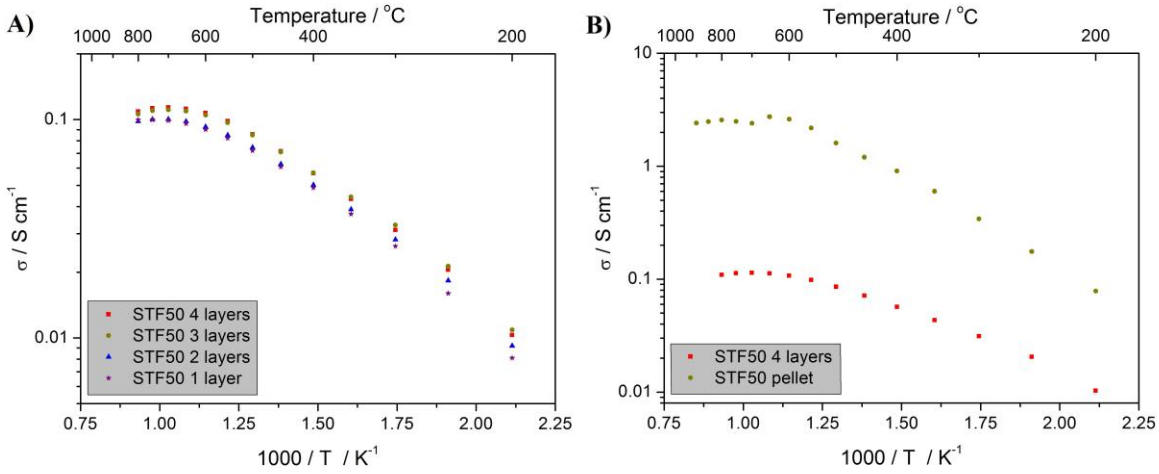


Figure 6. The STF50 DC conductivity of the samples with different number of the layers (A) and comparison with the pellet (B) measured at 21% $O_2$.

Post mortem SEM images of polished cross sections of porous STF35 layers with different thicknesses (n from 1 to 4) deposited on to $Al_2O_3$ substrates are shown at Fig. 7. All samples prepared by screen printing method and sintered at 800 °C, look similar. It has been calculated that one layer of screen printed STF compound had ~5.5 μm of

thickness after sintering. As presented, sintering at 800 °C reveals porous layer without cracks and with good adhesion to the substrate. It is a good perspective for typical SOFC electrolytes like YSZ, CGO because of smaller TEC mismatch. Namely, the used $Al_2O_3$ has TEC of 4.6 ppm $K^{-1}$ , while YSZ and CGO have of 10.8 ppm $K^{-1}$ and 12.3 ppm $K^{-1}$, respectively.

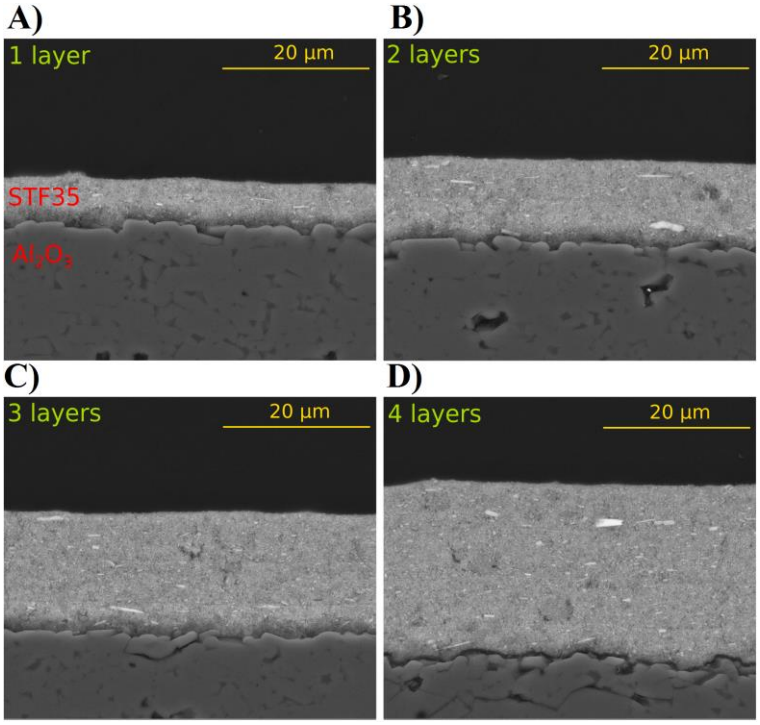


Figure 6. The SEM images of the polished cross section of the sintered at 800 °C STF35 porous layers with different thickness (A-B) on the $Al_2O_3$ substrate.

## Conclusions

For better understanding the role of the iron substitution on the performance of the $SrTi_{1-x}Fe_xO_3$ electrode, STF35, STF50 and STF70 were fabricated in a form of pellet and film and evaluated. All fabricated compounds had regular cubic structure and had no significant differences in size of powder particles or layers morphology (sintered at 800 °C) were observed. It was presented that despite of very high TEC differences of STF and the support, the films without cracks can be obtained.

Preliminary results of DC electrical conductivity measurements show that with increase of iron dopant there is an increase in conductivity and decrease of the activation energy. It was also found that porous layers had lower electronic conductivity than dense material and had lower activation energy. These preliminary results show that STF compounds with different iron dopant requires further electrochemical performance study.

## Acknowledgments

This work was supported by project funded by National Science Centre Poland "Understanding and minimization of ohmic and polarization losses in solid oxide cells by nanocrystalline ceramic and cermet functional layers (MiLoSoc)" based on decision 2017/25/B/ST8/02275.

## References

1. T. Chen, G. F. Harrington, K. Sasaki, and N. H. Perry, *ECS Trans.*, **75**, 23–31 (2017).
2. A. Mroziński, S. Molin, J. Karczewski, T. Miruszewski, and P. Jasiński, *Int. J. Hydrogen Energy*, **44**, 1827–1838 (2019).
3. R. A. De Souza, J. Fleig, R. Merkle, and J. Maier, *Zeitschrift für Met.*, **94**, 218–225 (2013).
4. R. A. Maier, C. A. Randall, and J. Stevenson, *J. Am. Ceram. Soc.*, **99**, 3350–3359 (2016).
5. V. Metlenko, W. Jung, S. R. Bishop, H. L. Tuller, and R. A. De Souza, *Phys. Chem. Chem. Phys.*, **18**, 29495–29505 (2016).
6. W. Jung and H. L. Tuller, *ECS Trans.*, **25**, 2775–2782 (2009).
7. W. Jung and H. L. Tuller, *ECS Trans.*, **35**, 2129–2136 (2011).
8. X. Yu, W. Long, F. Jin, and T. He, *Electrochim. Acta*, **123**, 426–434 (2014) http://dx.doi.org/10.1016/j.electacta.2014.01.020.
9. X. Yu, J. Fan, and L. Xue, *Ceram. Int.*, **40**, 13627–13634 (2014).
10. W. Jung and H. L. Tuller, *J. Electrochem. Soc.*, **155**, B1194 (2008) http://jes.ecsdl.org/cgi/doi/10.1149/1.2976212.
11. A. Nenning et al., *J. Electrochem. Soc.*, **164**, F364–F371 (2017) http://jes.ecsdl.org/lookup/doi/10.1149/2.1271704jes.
12. N. A. Baharuddin, A. Muchtar, M. R. Somalu, N. S. Kalib, and N. F. Raduwan, *Int. J. Hydrogen Energy* (2018).
13. E. O. Filatova et al., *Solid State Ionics*, **308**, 27–33 (2017) http://dx.doi.org/10.1016/j.ssi.2017.05.016.
14. A. Chrzan, J. Karczewski, M. Gazda, D. Szymczewska, and P. Jasinski, *J. Solid State Electrochem.*, **19**, 1807–1815 (2015).